Electronic Supplementary Material (ESI) for Materials Chemistry Frontiers.

Supplementary Information

Viologen Linker as a Strong Electron Transfer Mediator in Covalent Organic Framework to Enhance Electrocatalytic CO_2 Reduction

Xin Zhang,[1,2] Yin-Zong Yuan,[1,2] Hong-Fang Li,[2*] Qiu-Jin Wu,[2,3] Hong-Jing Zhu,[2,3] Yu-Liang Dong,[1,2] Qiao Wu,[2,3] Yuan-Biao Huang [2,3*] and Rong Cao [2,3,4*]

[1] College of Chemistry, Fuzhou University, Fuzhou, 350108, China

[2] State Key Laboratory of Structural Chemistry, Fujian Institute of Research on the Structure of Matter, Chinese Academy of Sciences, Fuzhou, 350002, Fujian

[3] University of Chinese Academy of Science, Beijing 100049

[4] Fujian Science & Technology Innovation Laboratory for Optoelectronic Information of China, Fuzhou, 350108, Fujian

[*]Corresponding Author(s): hongfangli@fjirsm.ac.cn; ybhuang@fjirsm.ac.cn; rcao@fjirsm.ac.cn

Content

S1. Materials and characterization methods

S1.1 Materials and Synthetic procedures

Chemicals:

All regents and chemicals were purchased from commercial sources without further purification. 1-Chloro-2,4-Dinitrobenzene (98%, Adamas), 4,4'-Bipyridine (98%, Aladdin), cobalt acetate tetrahydrate (99%, Aladdin), propionic acid (99%, J&K), $KHCO_3$ (99%, SCR), Carbon fiber paper (Toray) were purchased from the commercial.

Experimental Section:

(1)Synthesis of 5,10,15,20-tetrakis(4-cyanophenyl)porphyrin (TAPP):

Following a modified procedure from reference[S1].

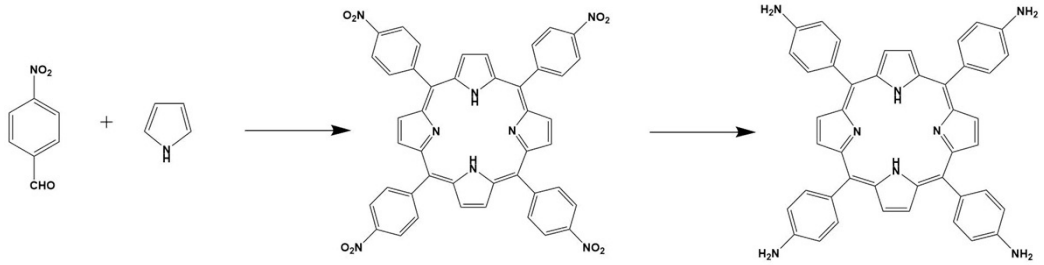

Scheme S1 Synthesis of TAPP

(1) Synthesis of 5,10,15,20-tetrakis (p-nitrophenyl)-21H, 23H-porphyrin (TNPP):

In a 500 mL flask, p-nitrobenzaldehyde (11 g, 0.07 mol), propionic acid (300 mL) and acetic anhydride (12 mL) were added and heated to 145 °C to reflux with stirring. Then the mixed solution with 5 mL of pyrrole and 10 mL of propionic acid was added and continued refluxing under stirring for 1 h. The mixed solution after that cooled to room temperature and stand undisturbed for 24 h. Then the crude product was affording through vacuum filtered, then washed with 100 mL water for 6 times. Put the crude product in a 80°C vacuum oven for overnight to drying to obtain purple-black solid. After that, the solid was mixed with 80 mL of pyridine and refluxed for 1 h, then cooled to room temperature and stored at -4 °C overnight to get black precipitate. Then the solvent was removed through vacuum filtered and washed the filter cake with acetone for several times until the filtrate become colorless, yielding bright purple product TNPP.

(2) Synthesis of 5, 10, 15, 20-tetrakis (para-aminophenyl)-21H, 23H-porphyrin (TAPP):

2.2 g of TNPP was dissolved in 100 mL of concentrated hydrochloric acid. 25 mL of concentrated hydrochloric acid solution containing 9.3 g of $SnCl_2 \cdot 2H_2O$ was added dropwise to the porphyrin solution within 10 min at room temperature under stirring, and then the temperature was raised to 70 °C for 1h. The dark green solid was separated by ice bath cooling, the hydrochloride was dispersed in 200 mL of deionized water, neutralized with concentrated ammonia to pH = 9, and the solid was collected by centrifugation and dried under vacuum at 70 °C. The product was extracted with 300 mL chloroform by using a Soxhlet extractor, and solvent was concentrated to 20 mL by rotary evaporation, it was recrystallized by adding 100 mL of diethyl ether to obtain of bright purple TAPP crystal. ^{1}H NMR (DMSO, 400 MHz): δ ppm 8.88 (s, 8H, pyrrole-C-H), 7.85 (d, J =8.1 Hz, 8H, Ar-H), 7.00 (d, J = 8.1 Hz, 8H, Ar-H), 5.58 (s, 8H, NH_2), -2.75 (s, 2H, pyrrole-N-H) (Fig. S1), consistent with literature reports[S2].

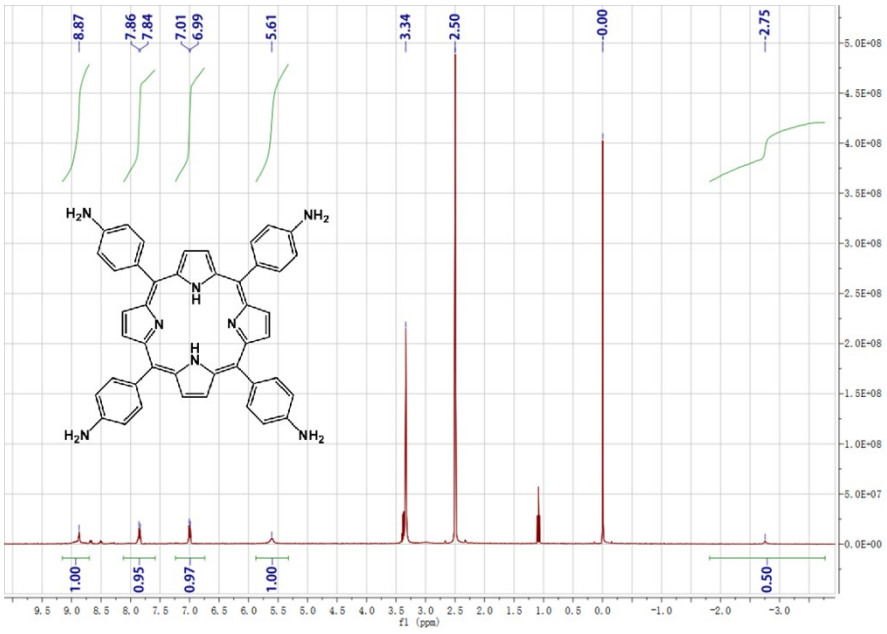

Fig. S1 ^{1}H NMR spectrum of TAPP.

Synthesis of 5,10,15,20-tetrakis(4-aminophenyl)-porphinatocobalt (Co-TAPP)

Co-TAPP was synthesized according to reference and slightly modified. TAPP (200 mg, 0.30 mmol) and NaOAc (108 mg, 1.3 mmol) were added mixed solution with 63 mL of chlorobenzene and 45mL of DMF, then $Co(OAc)_2 \cdot 4H_2O$ (200 mg, 0.3 mmol) was added. After equipping with a Soxhelt apparatus with a paper thimble containing K_2CO_3 (1.1 g, 8.0 mmol), the reaction mixture was stirred under nitrogen at reflux for 24 h. Upon cooling, the Soxhlet apparatus was replaced with a distillation setup, and the solvent was removed under vacuum. The resulting dark solid

was suspended in $CHCl_3$ (100 mL) and transferred to a Buchner funnel with a glass frit, and the solvent was removed through vacuum filtration. The crude product was then washed thoroughly with water three times, saturate $NaHCO_3$ solution one times, and then water again three times. The resulting dark purple microcrystalline powder was dried under high vacuum overnight. The Q-band between 500 ~ 700 nm is reduced to two characteristic peaks, and the Soret band shows a certain degree of blue shift, which is the most obvious feature of forming UV-Vis spectrum of metallic porphyrins (Fig. S2).

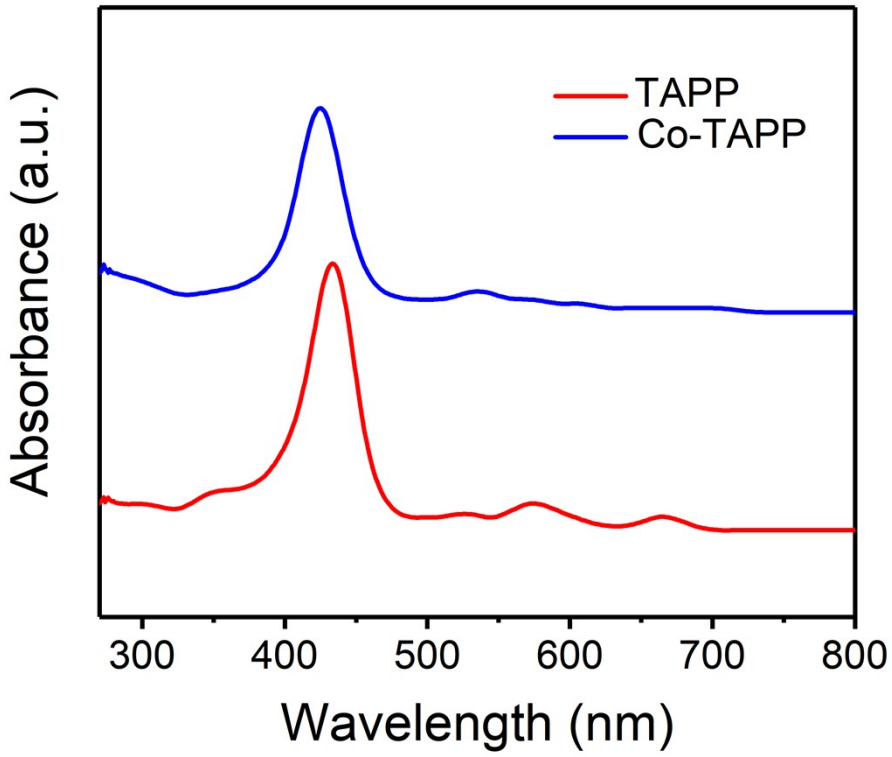

Fig. S2 UV-Vis absorption spectra of TAPP (red line) and Co-TAPP (blue line)

Synthesis of TNV

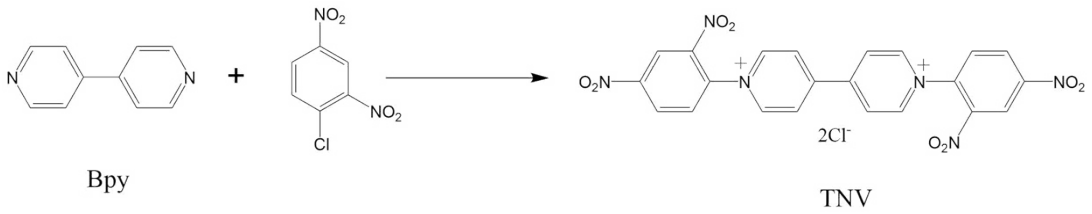

Scheme S2 Synthesis of TNV.

1,1'-bis(2,4-dinitrophenyl)-[4,4'-bipyridine]-1,1'-diium dichloride (tetranitroviologen, TNV, 2) was synthesized by refluxing 4,4'-bipyridine (0.8 g, 5 mmol) and 1-chloro-2,4- dinitrobenzene (3.5

g, 15 mmol) in 150 mL of anhydrous acetonitrile under Ar for 72 h. After the reaction was complete, the mixture was filtered, and the solid was washed with acetonitrile (50 ml, once) and diethyl ether (40 ml, four times, followed by soaking). Pure TNV was obtained in 75% yield. ^{1}H NMR (400 MHz, MeOD δ): δ 9.46 (d, 4H), 9.39 (d, 2H), 8.90–8.94 (m, 6H), 8.29 (d, 2H) ppm (Fig. S3). ^{13}C NMR (126 MHz, D_2O) δ 152.66, 149.89, 146.86, 142.82, 138.24, 131.10, 130.75, 127.55, 122.82 ppm (Fig. S4).

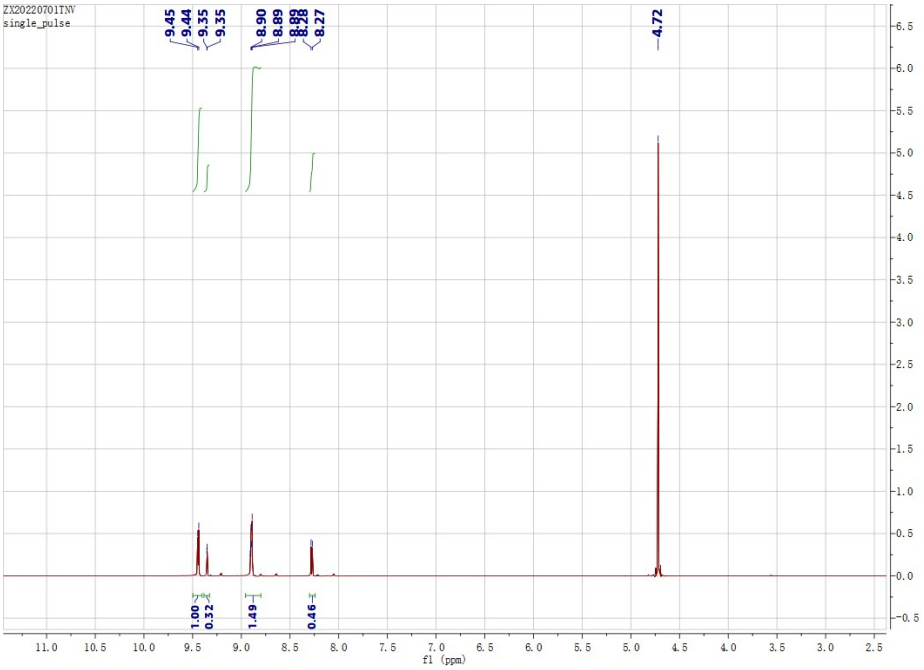

Fig. S3 ^{1}H NMR spectrum of TNV.

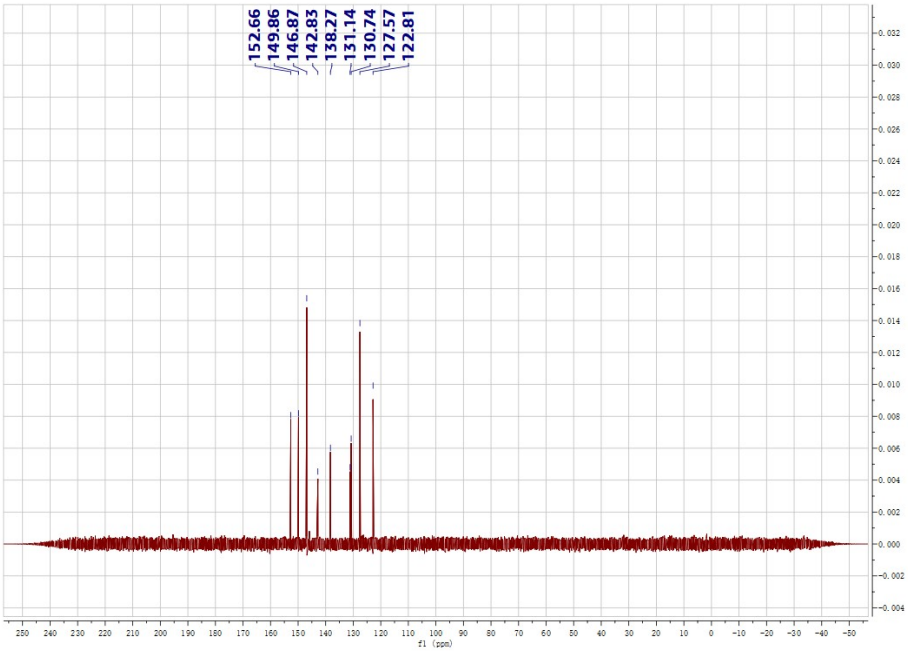

Fig. S4 ^{13}C NMR spectrum of TNV.

Synthesis of Por(Co)-Vg-COF

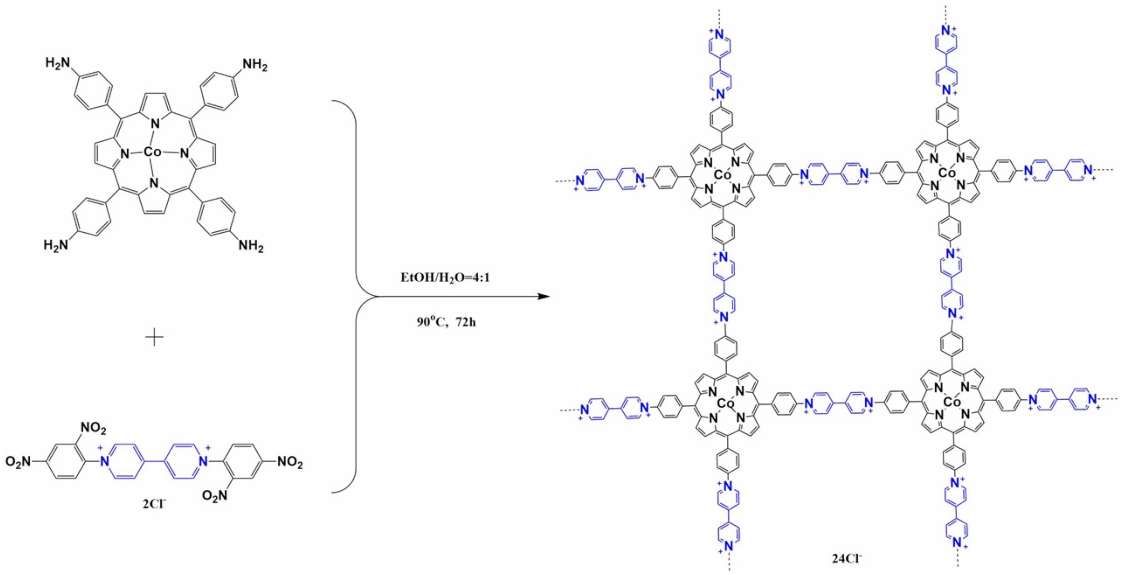

Scheme S3. Synthesis of Por(Co)-Vg-COF

A mixture of Co-TAPP (15 mg, 0.02 mmol), TNV (22.17 mg, 0.04 mmol), anhydrous ethanol (1.6 mL) and H_2O (0.4 mL) were dissolved in a Pyrex tube (outside diameter × length, 8 × 198 mm). After sonication for about 15 min, the tube was flash frozen at 77 K (liquid N_2 bath) and degassed to achieve an internal pressure of ~100 mTorr. After the temperature recovers to room temperature, the mixture was heated at 90 °C and left undisturbed for 72 h. The obtained solid was repeatedly washed with ethanol until the supernatant appeared clear. The solid product was dried overnight in a vacuum oven at 70 °C.

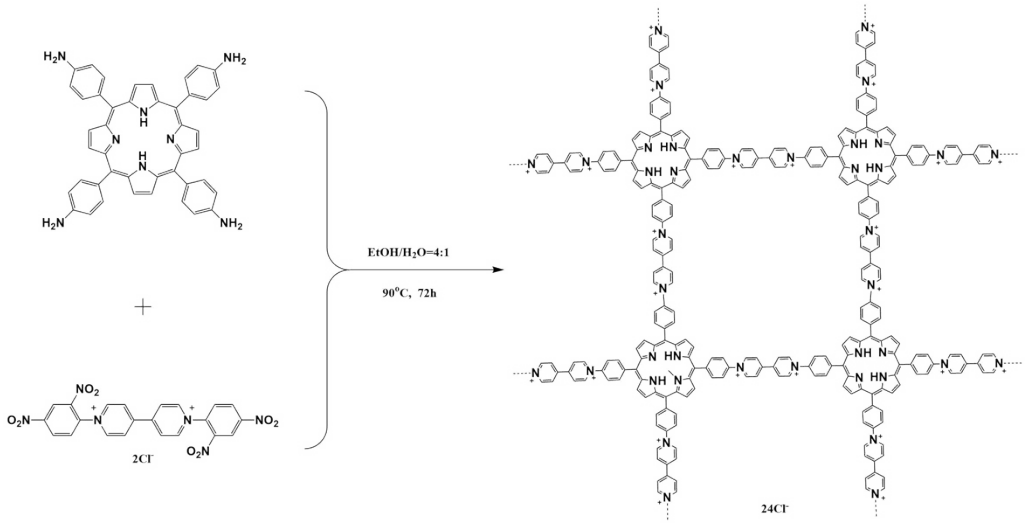

Scheme S4 Synthesis of Por(H)-Vg-COF.

A mixture of TAPP (15 mg, 0.02 mmol), TNV (22.17 mg, 0.04 mmol), anhydrous ethanol (1.6 mL) and H_2O (0.4 mL) were dissolved in a Pyrex tube (outside diameter × length, 8 × 198 mm). After sonication for about 15 min, the tube was flash frozen at 77 K (liquid N_2 bath) and degassed

to achieve an internal pressure of ~100 mTorr. After the temperature recovers to room temperature, the mixture was heated at 90 °C and left undisturbed for 72 h. The obtained solid was repeatedly washed with ethanol until the supernatant appeared clear. The solid product was dried overnight in a vacuum oven at 70°C.

Characterization methods.

A Micrometrics ASAP 2020 instrument was used to measure CO_2 adsorption-desorption isotherms. Powder X-ray diffraction (PXRD) patterns were recorded on a Miniflex 600 diffractometer using Cu Kα radiation (λ = 0.154 nm). X-ray photoelectron spectroscopy (XPS) measurements were performed on an ESCALAB 250Xi X-ray photoelectron spectrometer (Thermo Fisher) using an Al Ka source (15 kV, 10 mA). The analysis of Co content in the samples was measured by Inductively Coupled Plasma Atomic Emission Spectroscopy (ICP-AES) using an Ultima 2 analyser (Jobin Yvon). Transmission electron microscope (TEM) images were taken on an FEI TECNAI G2 F20 microscope equipped with an EDS detector at an acceleration voltage of 200 kV. XAFS measurement and data analysis: At the BL14W1 station of the Shanghai Synchrotron Radiation Facility (SSRF), XAFS spectra were collected at the Co-K edge. The transmission mode was used to record the Co K-edge XANES data. For the faradaic efficiency analysis, gas products were detected by gas chromatograph (Agilent 7820A) and liquid product was characterized by ^{1}H NMR on Bruker AVANCE AV Ⅲ 400. The Nyquist plots were obtained by electrochemical impedance spectroscopy (EIS) measurement carried out by applying an AC voltage of 5 mV amplitude in the frequency range 0.01 Hz to 100 kHz with 0.5 M Na_2SO_4 electrolyte. In situ Fourier transform infrared spectroscopy was provided by Thermo Snow. Gas chromatography-mass spectrometry (GC-Mass) was provided by Shimazu QP2020.

S1.2 Electrical conductivity measurements

To make a pressed pellet, the MOF sample was put into a 6 mm inner-diameter split sleeve pressing die and pressed for 5 min under a pressure of approximately 1000 psi. A two-contact probe method was employed to collect bulk conductivity measurements of the MOFs pellet. The two-contact probe method is easy to configure and is suitable for the conductivity measurement of resistive samples. We calculated the bulk conductivity measurements (S/cm) using the following equations. Herein, L is the distance of between the probes, which equals the thickness of the pellet, A is the basal area of the pellet, V (volts) is the voltage of cross the probes, I (A) is

current, which is measured by a potentiostat.

$$\sigma = \frac{IL}{VA}$$

S2. Electrochemical measurements

H-type cell:

The electrochemical measurements were performed in a H-type cell with two-compartments separated by an anion exchange membrane (Nafion-117) by chi700e at room temperature. One compartment contained 70 mL electrolyte (0.5 M $KHCO_3$ aqueous solution made from DI water) and Pt foil as counter electrodes, another with the same electrolyte, Ag/AgCl electrode in saturated KCl solution as reference electrodes and working electrode. Typically, 5 mg of the catalyst was dispersed in 500 μL of isopropanol and 20 μL of Nafion binder solution (5 wt%) under sonication for 1 h to form a homogeneous ink. Then 1 μg of cobalt was loaded onto the carbon fiber paper electrode with 1×1 cm^2. During the electrochemical measurements, the electrolyte solution was purged with CO_2 for 30 min to achieve the CO_2-saturated solution. Linear sweep voltammetry (LSV) was performed with a scan rate of 10 mV s^{-1} in N_2-saturated or CO_2-saturated 0.5 M $KHCO_3$ electrolyte. All measured potentials were converted to reversible hydrogen electrode (RHE) scale using the following equation: E(vs. RHE) = E(vs. Ag/AgCl)+ 0.059 pH + 0.197 V. CO_2 gas was delivered at an average rate of 30 mL/min (at room temperature and ambient pressure) and routed into the gas sampling loop (1 mL) of a gas chromatograph. The gas phase composition was analyzed by GC every 8 min. The separated gas products were analyzed by a thermal conductivity detector (for H_2) and a flame ionization detector (for CO, CH_4). The liquid products were analyzed afterwards by quantitative NMR (Bruker AVANCE AV Ⅲ 400) using dimethyl sulphoxide (DMSO) as an internal standard.

Flow cell:

Electrochemical measurements with high current densities were performed in a flow cell consists of a gas diffusion electrode (GDE), an anion exchange membrane and a carbon paper gas diffusion layer (GDL) anode. 100 μL catalyst ink was loaded onto a 1 cm × 3 cm GDL to create a GDE. The homogeneous ink was prepared using 5 mg of catalyst and 2.5 mg ketjenblack

dispersed into 500 μL of isopropanol containing 20 μL Nafion solution (5 wt%). An Ag/AgCl was acted as the reference. Two kinds of electrolyte 1 M KOH aqueous solution and 0.005 M H_2SO_4 with a 0.05 M K_2SO_4 additive aqueous solution were used and was circulated through the anode side using a peristaltic pump. CO_2 gas was supplied to the cathode side with a constant flow rate of 30 ml min^{-1} monitored by a flow controller. Linear sweep voltammetry (LSV) was performed with a scan rate of 10 mV s^{-1}. In the studies, all potentials were converted to potential vs. reversible hydrogen electrode (RHE) according to the equation E (vs. RHE) = E (vs. Ag/AgCl) + 0.1989 V + 0.059 × pH. During electrolysis procedure, the effluent gas from the cathode compartment went through the sampling loop (1 mL) of a gas chromatograph. The gas phase composition was analyzed by GC every 8 min. The separated gas products were analyzed by a thermal conductivity detector (for H_2) and a flame ionization detector (for CO).

S3. Supporting Figures and Tables

Table S1 ICP results of Por(Co)-Vg-COF.

Sample	Por(Co)-Vg-COF
Co	2.43 wt%

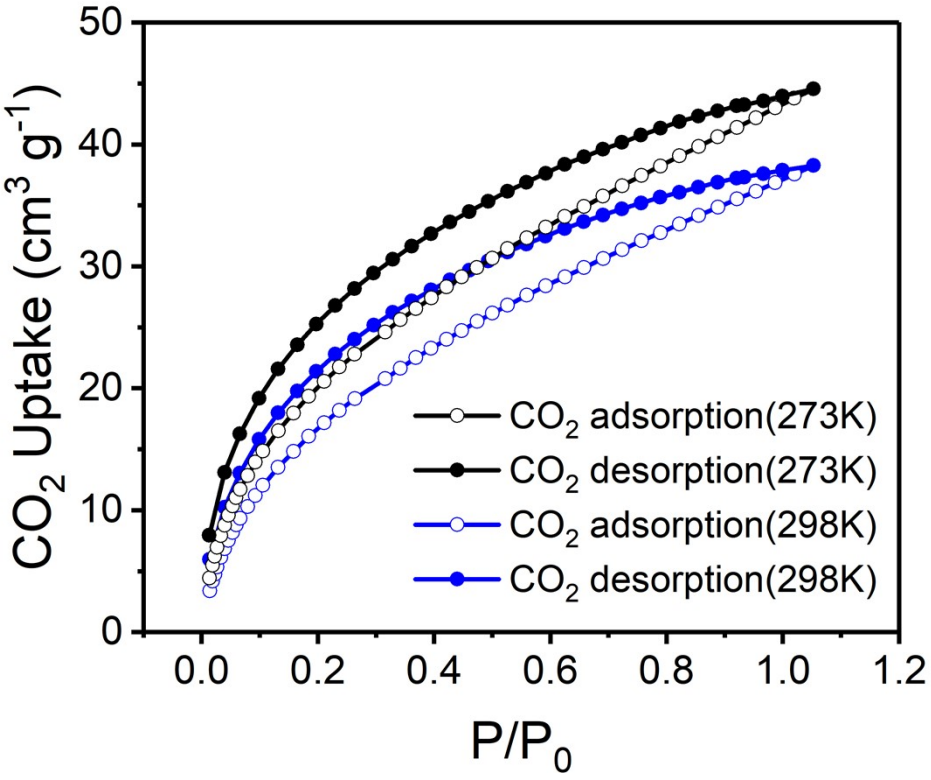

Fig.S5 CO_2 sorption of Por(Co)-Vg-COF measured at 273 K (black line) and 298 K (blue line), respectively.

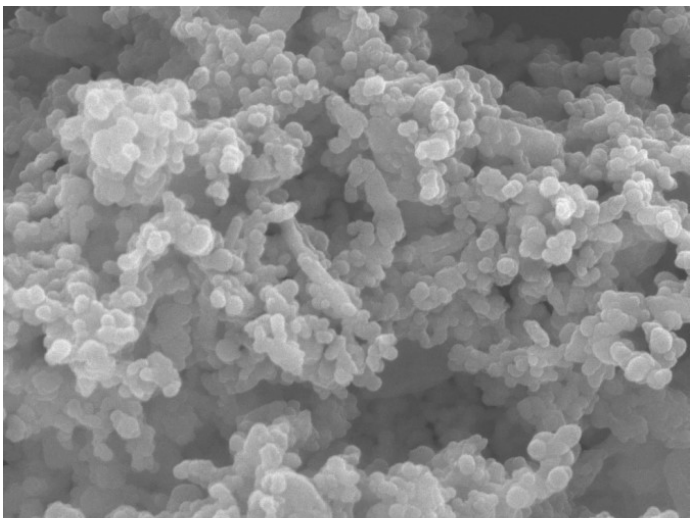

Fig. S6 SEM images of Por(Co)-Vg-COF.

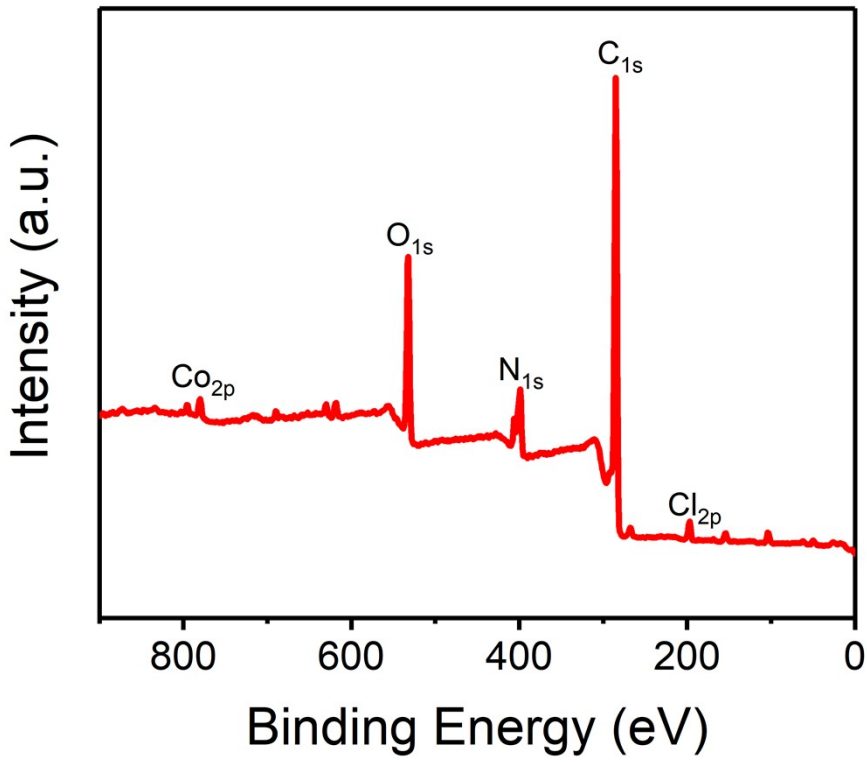

Fig. S7 Survey XPS spectra of Por(Co)-Vg-COF.

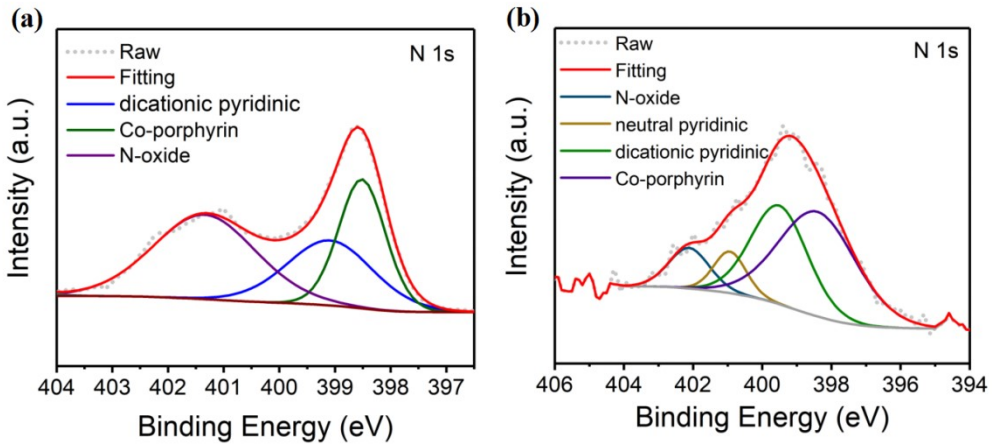

Fig. S8 The XPS N 1s spectra of Por(Co)-Vg-COF catalysis before (a) and (b) after CO_2RR.

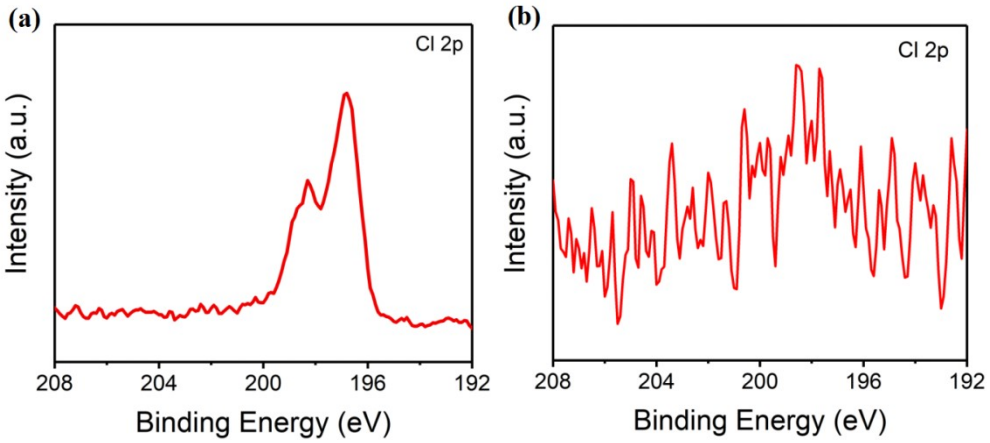

Fig. S9 The XPS Cl 2p spectra of Por(Co)-Vg-COF catalysis before (a) and (b) after CO_2RR.

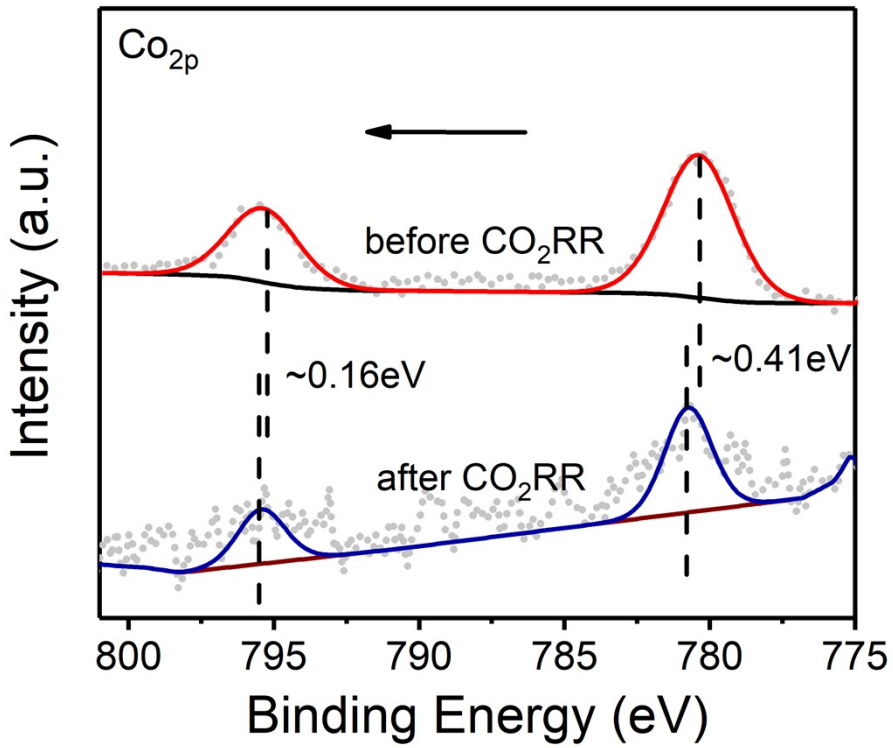

Fig. S10 The XPS Co 2p spectra of Por(Co)-Vg-COF catalysis before and after CO_2RR.

Table S2 Fitting results based on EXAFS analysis of Por(Co)-Vg-COF.

Sample	Path	CN	R(Å)	$\sigma^2(10^{-3}Å^2)$	R factor
Por(Co)-Vg-COF	Co-N	4.5	1.95	0	0.030

CN: coordination number; σ^2:Debye-Waller factor (a measure of thermal and static disorder in absorber-scatterer distances); $\triangle$E0: the inner potential correction; R factor is used to value the

goodness of the fitting.

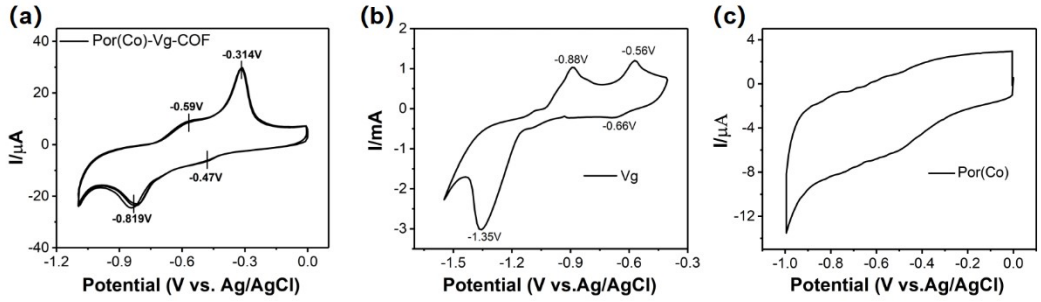

Fig. S11 Cyclic voltammograms of (a) Por(Co)-Vg-COF; (b) Vg; (c) Por(Co).

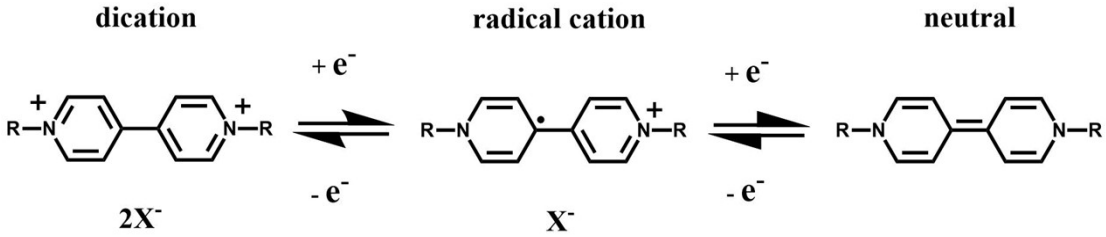

Scheme S5 Redox chemistry of viologen.

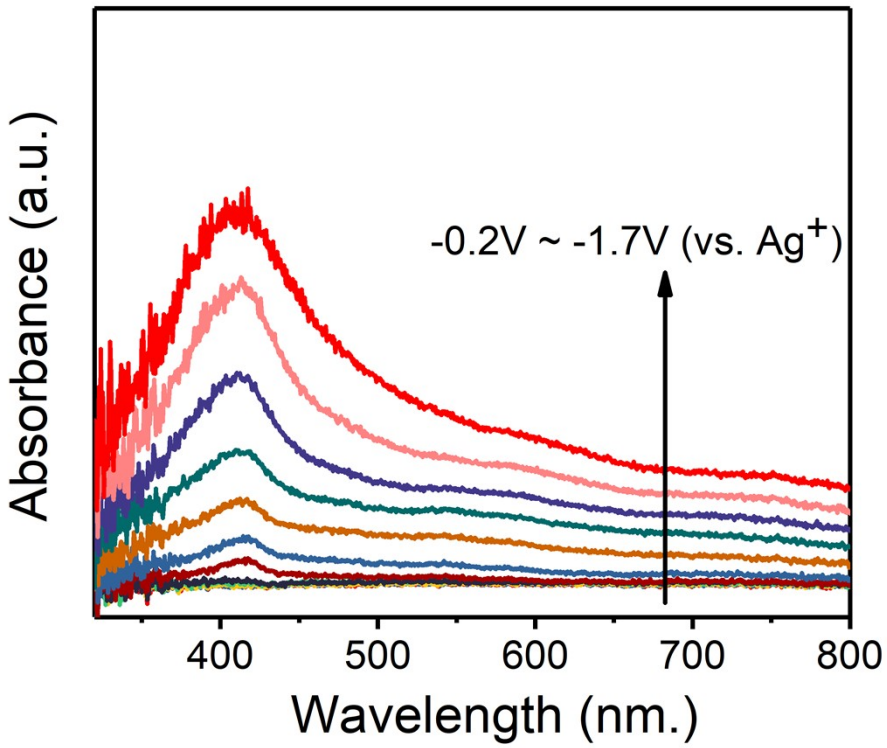

Fig. S12 UV-Vis spectra of Por(Co)-Vg-COF in 0.2 M Na_2SO_4 aqueous solution recorded during reductive spectroelectrochemical measurements (The background is the material without voltage).

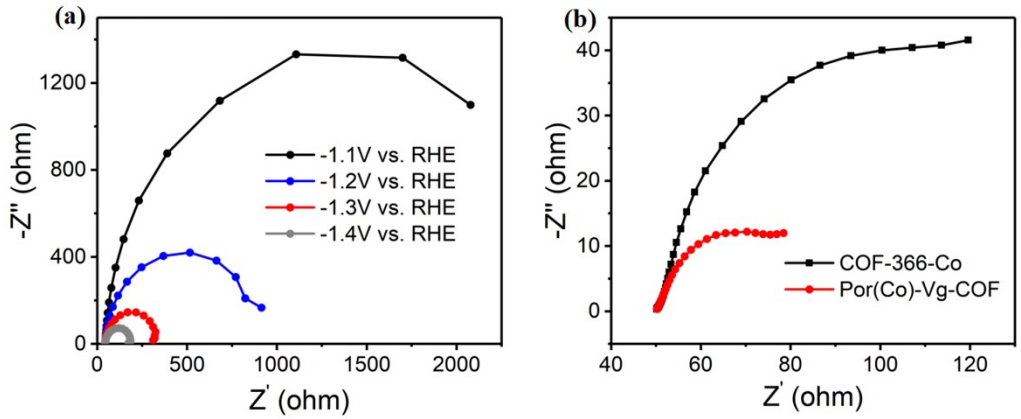

Fig. S13 (a) Nyquist plots from −1.1 to −1.4 V of Por(Co)-Vg-COF. (b) Nyquist plots of Por(Co)-Vg-COF and COF-366-Co.

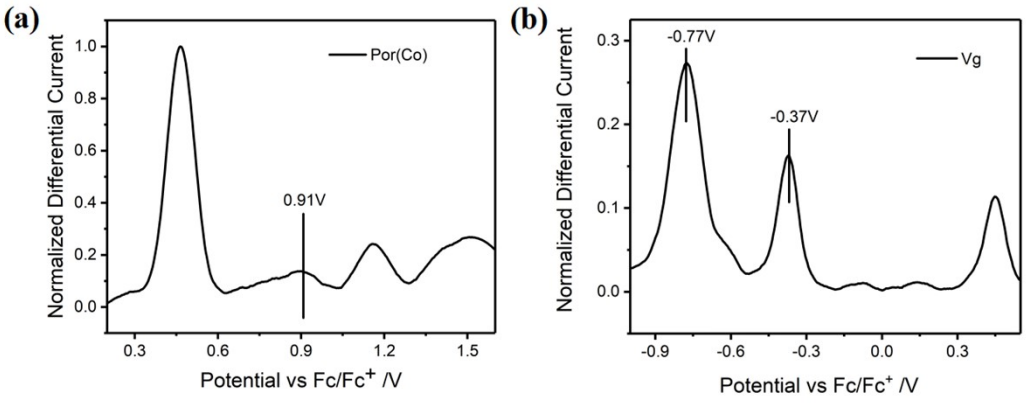

Fig. S14 Differential pulse voltammetry (DPV) measurements on (a) Por(Co) and (b) Vg referenced to ferrocene at 0.45V.

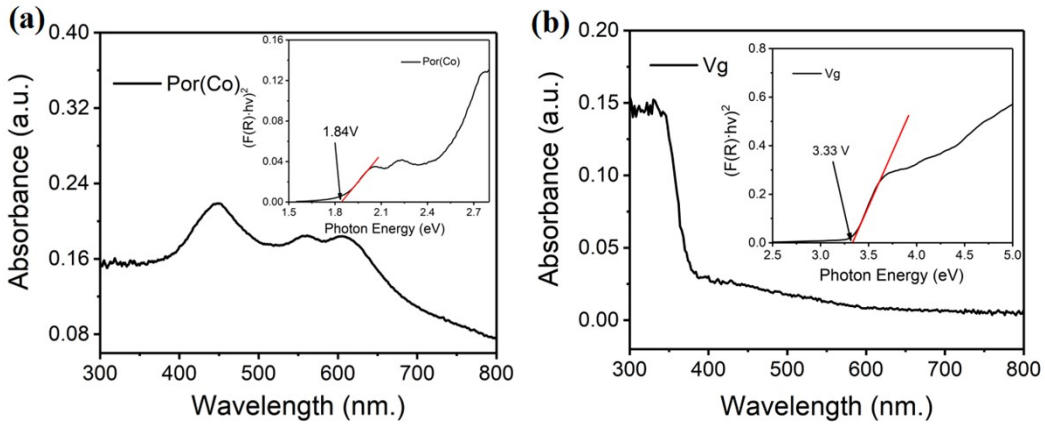

Fig. S15 Solid state UV-Vis spectra (inset Tauc plot) of a) Por(Co), and b) Vg.

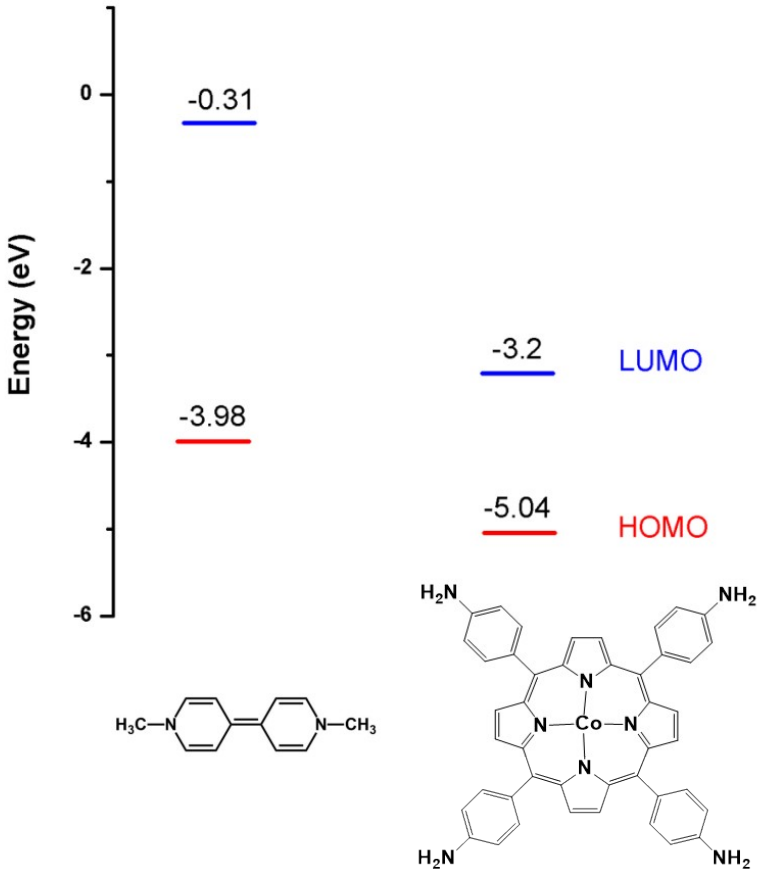

Fig. S16 Relevant energy levels of the monomers with HOMO (red) and LUMO (blue), which were determined by combining differential pulse voltammetry measurements and UV-vis data.

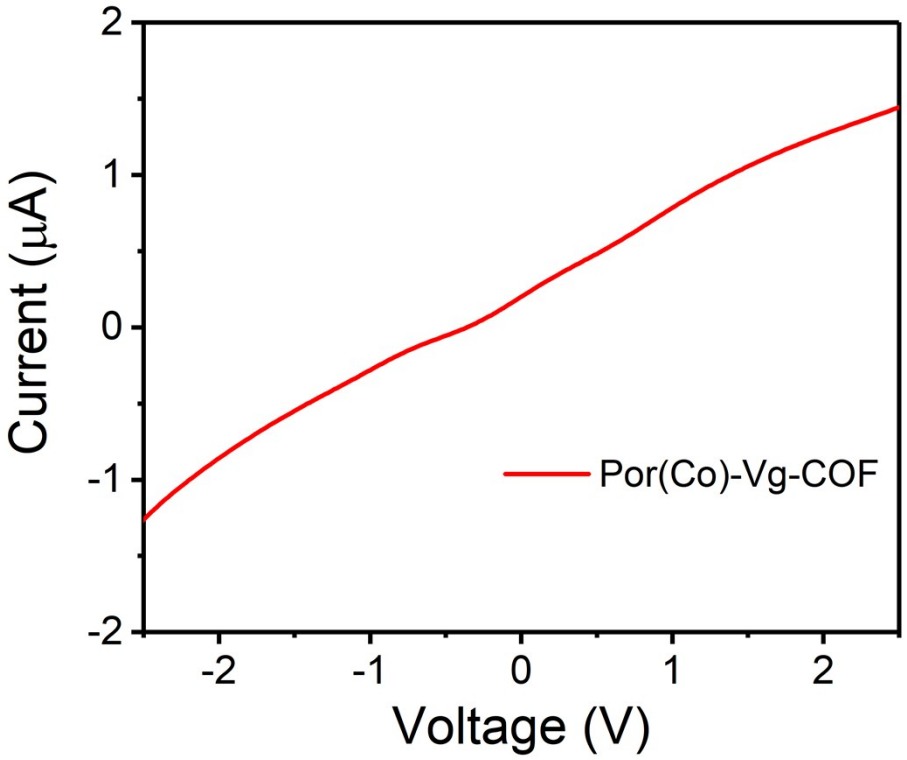

Fig. S17 Electrical measurement of Por(Co)-Vg-COF was performed using two-electrode in air at a constant temperature of 298 K and in the absence of light. The Por(Co)-Vg-COF electrical conductivity is calculated to be 3.7×10^{-7} S.cm^{-1} ($\sigma = L/(R\times\pi(d/2)^2)$), L = 0.51 mm, d = 2.5 mm, R = 1.7906×10^{6} Ω).

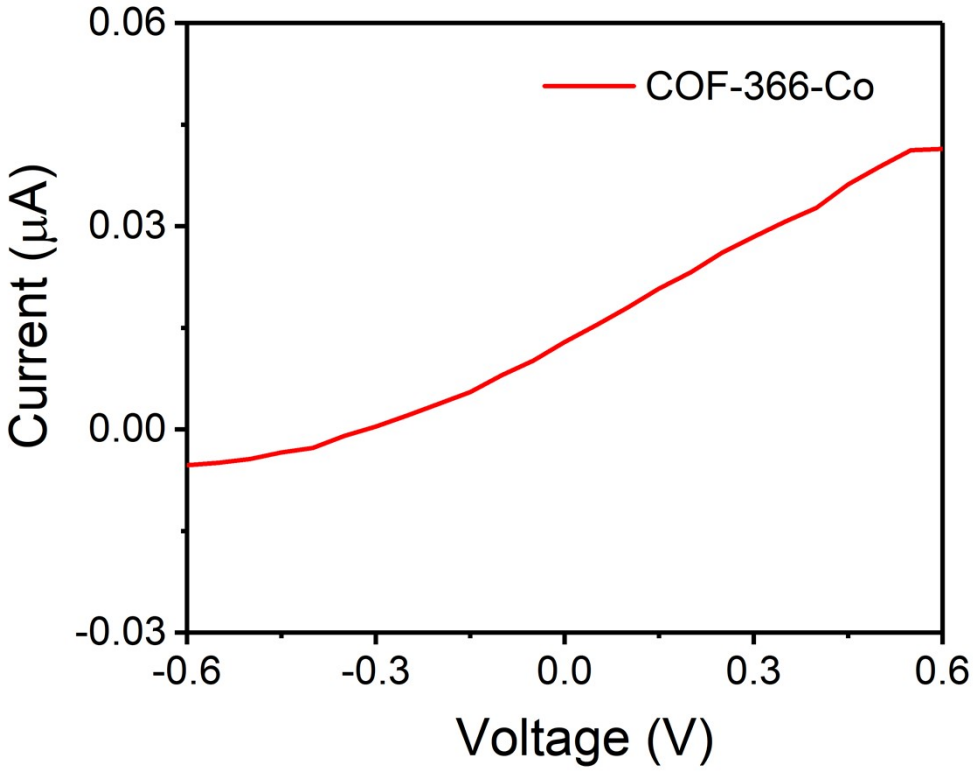

Fig. S18 Electrical measurement of COF-366-Co was performed using two-electrode in air at a constant temperature of 298 K and in the absence of light. The COF-366-Co electrical conductivity is calculated to be 2.08×10^{-7} S.cm^{-1} ($\sigma = L/(R\times\pi(d/2)^2)$), L = 0.506 mm, d = 2.5 mm, R = 4.9479×10^{7} Ω).

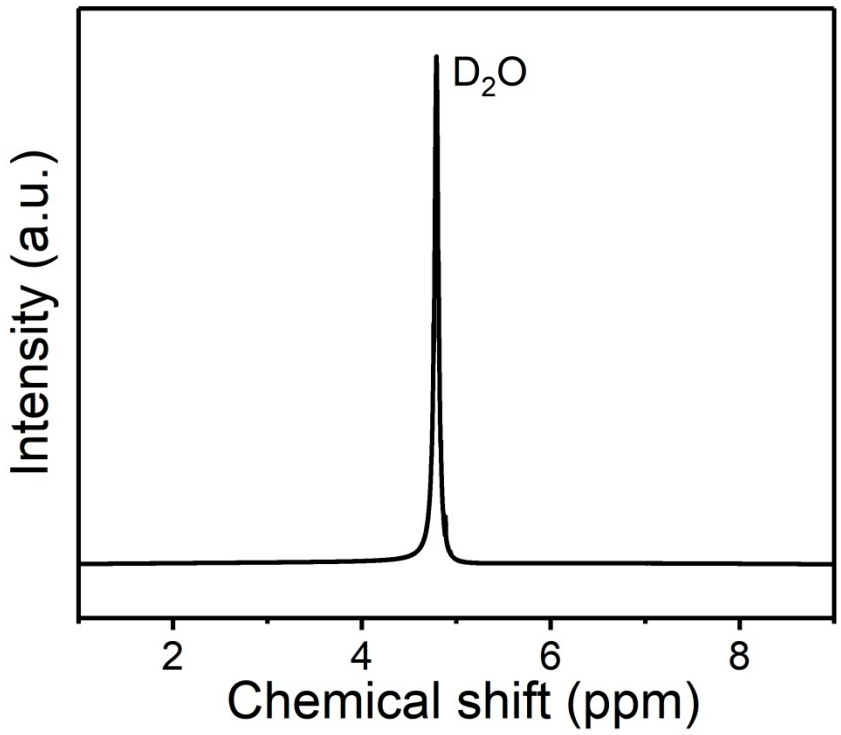

Fig. S19 ^{1}H NMR spectra of Por(Co)-Vg-COF for the electrolyte test after CO_2RR at –0.6 V vs RHE in 0.5 M $KHCO_3$.

Table S3 Comparison of CO Faradaic efficiency of various catalysts for CO_2 electroreduction.

Catalyst	**Electrolyte**	**Applied potential (V vs RHE)**	**Optimal FE_{CO} (%)**	**Highest J_{CO} [mA cm^{-2}]**	**Ref.**
Por(Co)-Vg-COF	**0.5 M $KHCO_3$**	**-0.6**	**98.54**	**18.8 (-1.1 V)**	**This work**
COF-366-Co	0.5 M $KHCO_3$	-0.7	89.9	10.35 (-0.9 V)	This work
COF-367-Co	0.5 M $KHCO_3$	-0.67	91	3 (-0.67	1

				V)	
COF-366-Co(10%)	0.5 M $KHCO_3$	-0.67	70	0.56 (-0.67 V)	1
COF-366-Co(1%)	0.5 M $KHCO_3$	-0.67	40	0.16 (-0.67 V)	1
Co-TTCOF	0.5 M $KHCO_3$	-0.7	91.3	~4.25 (-0.9 V)	2
TTF-Por(Co)-COF	0.5 M $KHCO_3$	-0.7	95	~6.88 (-0.9 V)	3
TT-Por(Co)-COF	0.5 M $KHCO_3$	-0.6	91.4	7.28 (-0.7 V)	4
COF-366-F-Co	0.5 M $KHCO_3$	-0.67	87	65 mA mg^{-1} (-0.67 V)	5
COF-300	0.5 M $KHCO_3$	-0.85	27	~0.12 (-0.85 V)	6
COF-300-AR	0.5 M $KHCO_3$	-0.85	80	~1.75 (-0.85 V)	7
F5-PCN-222(Fe)	0.5 M $KHCO_3$	-0.7	97	3.36 (-0.8)	8
3D-Por(Co/H)-COF	0.5 M $KHCO_3$	-0.6	92.4	15.5 (-1.1)	9

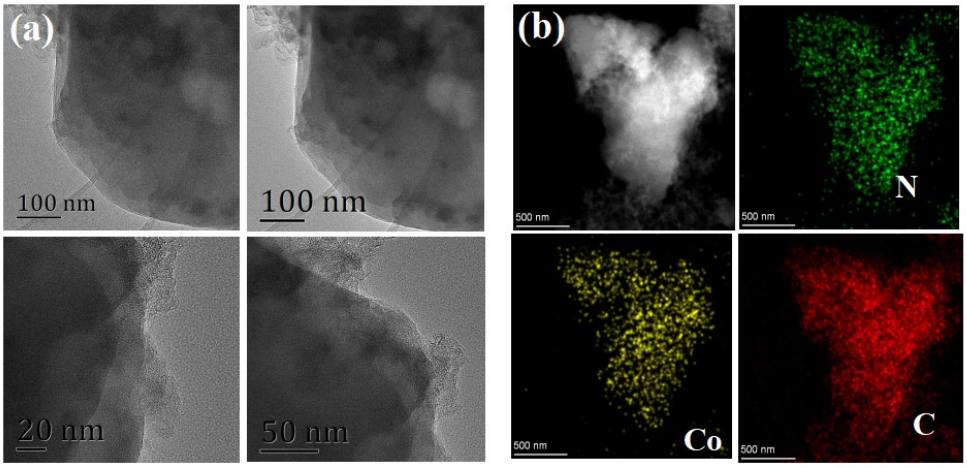

Fig. S20 a) TEM image of Por(Co)-Vg-COF after CO_2RR testing. b) HAADF-STEM image and the corresponding C, N, and Co EDS elemental mappings after CO_2RR testing.

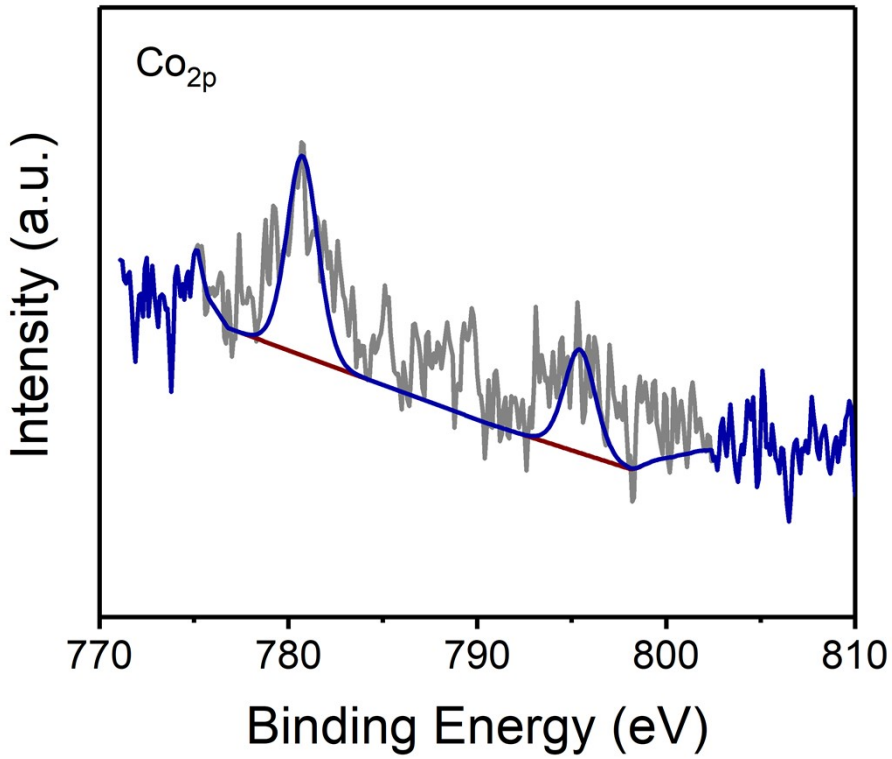

Fig. S21 The XPS Co 2p spectra of Por(Co)-Vg-COF after catalysis.

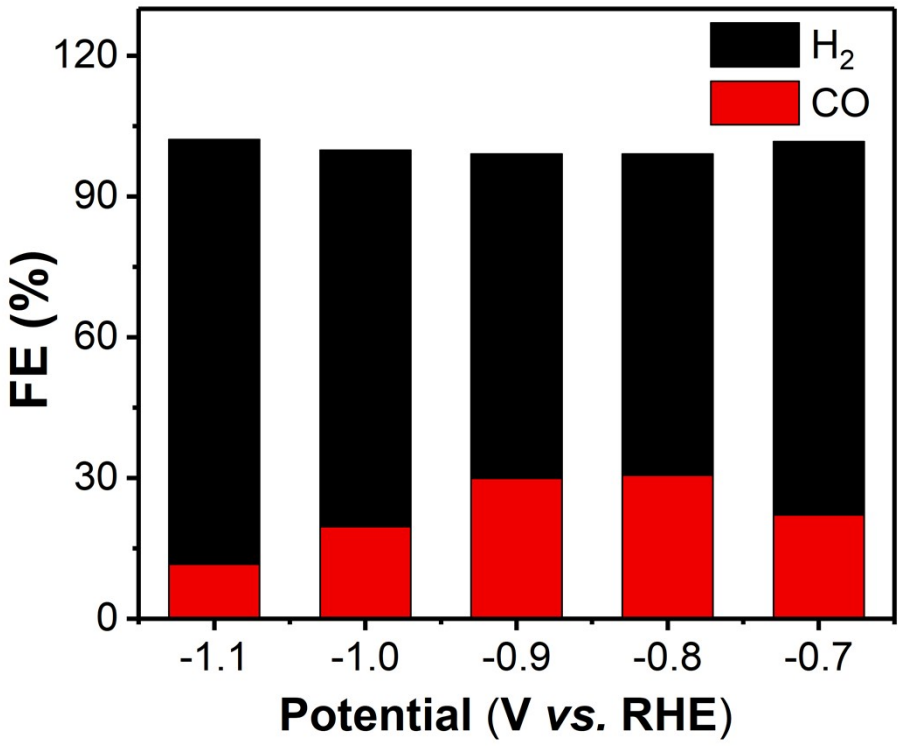

Fig. S22 FE_{CO} and FE_{H2} from −0.7 to −1.1 V versus RHE of Por(H)-Vg-COF.

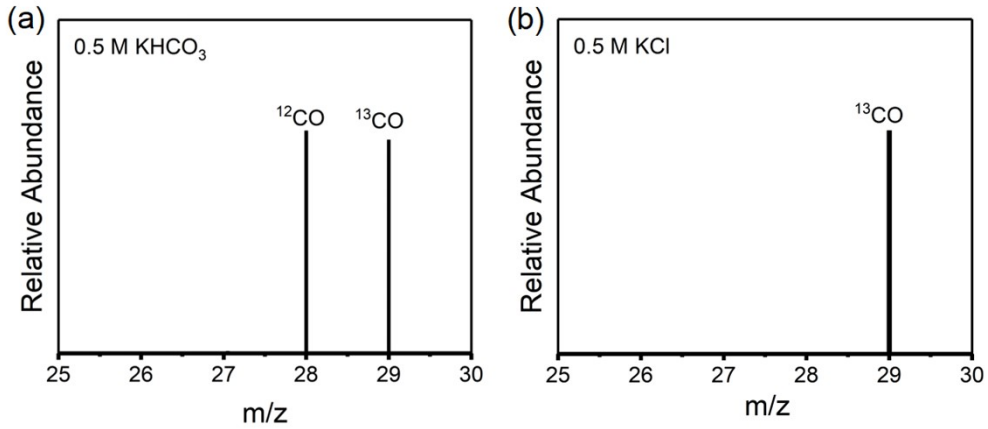

Fig. S23 Mass spectra of Por(Co)-Vg-COF in the $^{13}CO_2$-saturated (a) 0.5 M $KHCO_3$ and (b) 0.5 M KCl.

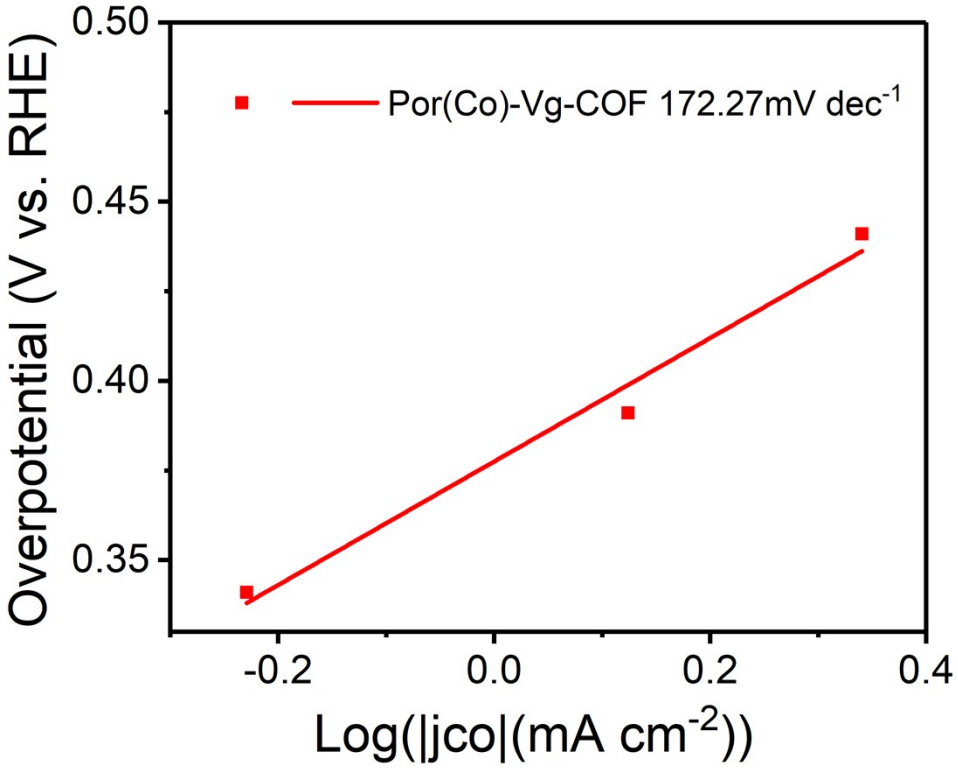

Fig. S24 Tafel plots of Por(Co)-Vg-COF.

Table S4 ICP results of acidic/alkaline aqueous electrolyte after CO_2RR of Por(Co)-Vg-COF.

Sample	acidic	alkaline
Co (mg/L)	0.032	0.0106

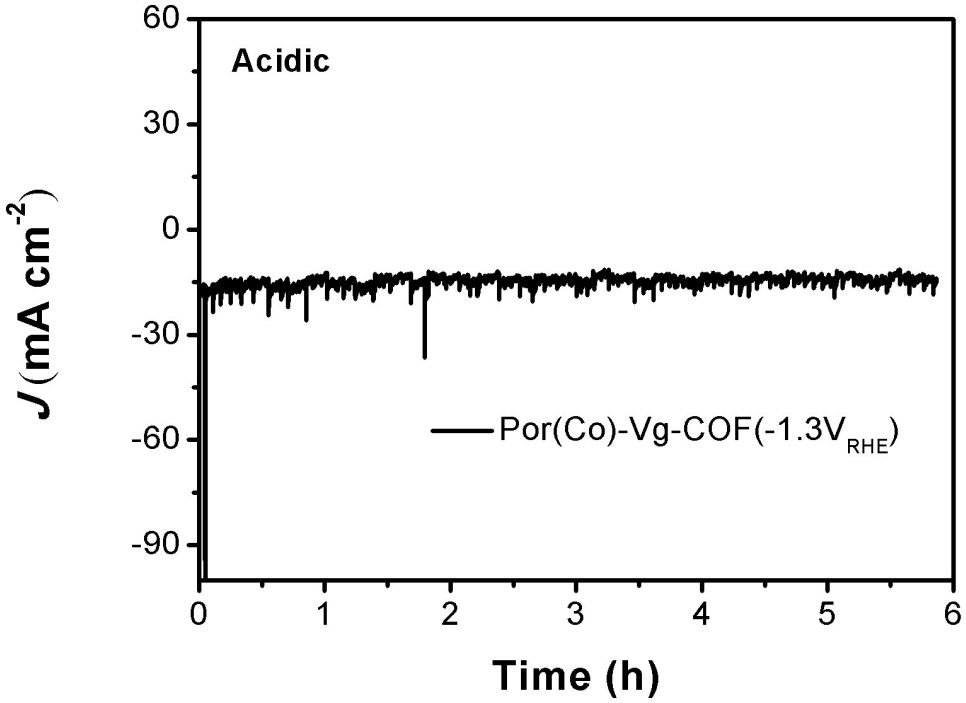

Fig. S25 Stability test (total current density) at −1.3 V for 6 h in 0.06 M H_2SO_4 with 0.5 M K_2SO_4 addictive aqueous electrolyte.

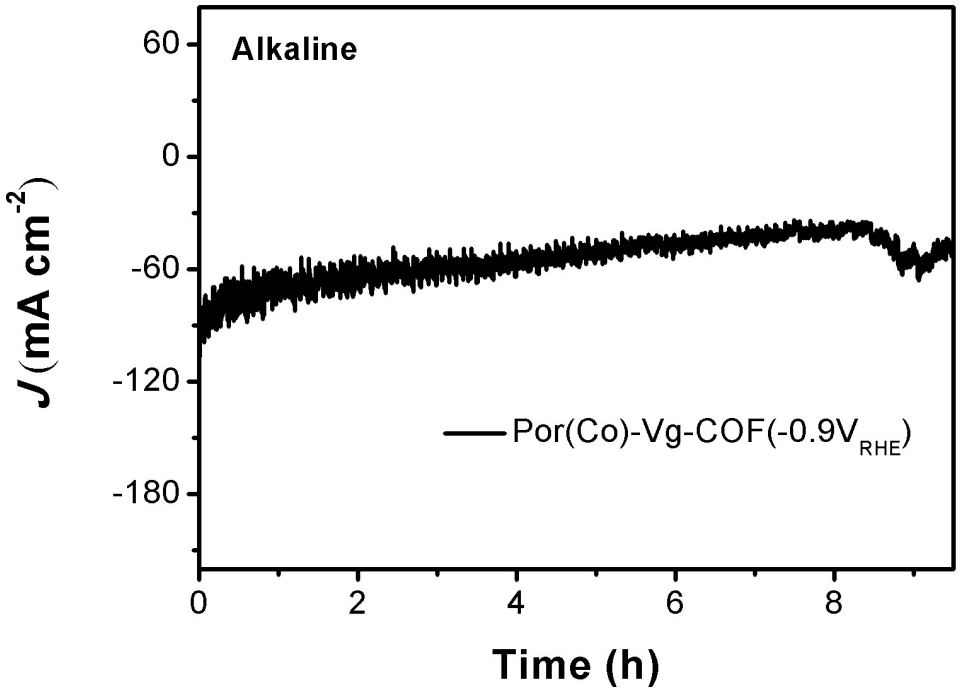

Fig. S26 Stability test (total current density) at −0.9 V for 9.5 h in 1 M KOH aqueous electrolyte.

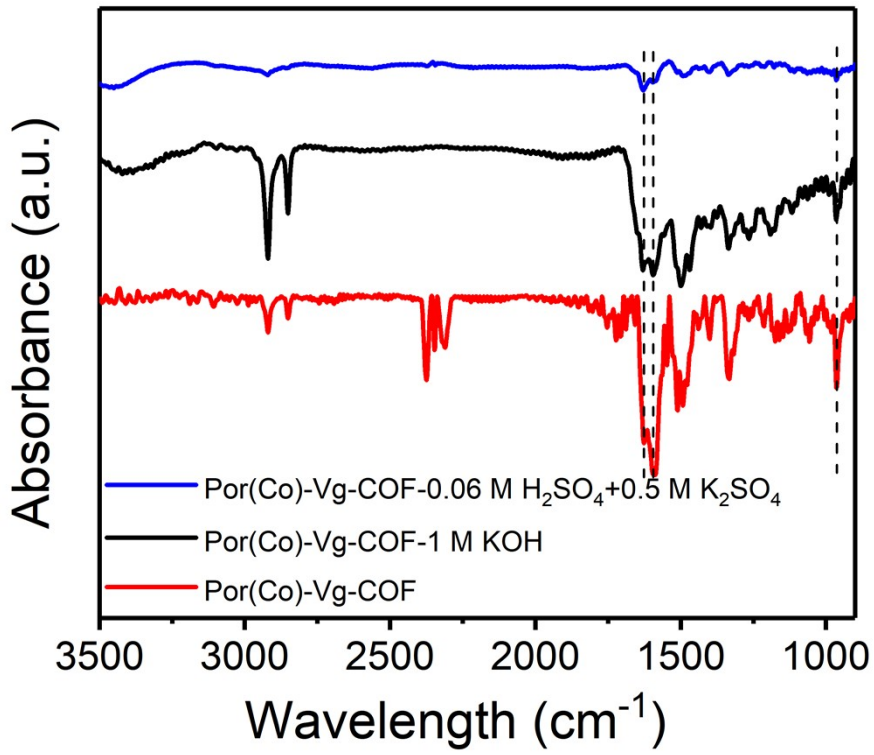

Fig. S27 The comparison of FT-IR spectra of Por(Co)-Vg-COF (red curve) and after immersed 4 hours in 0.06 M H_2SO_4 with 0.5 M K_2SO_4 additive (blue curve) and 1 M KOH (black curve), respectively.

S4. References

1 S. Lin, C. S. Diercks, Y.-B. Zhang, N. Kornienko, E. M. Nichols, Y. Zhao, A. R. Paris, D. Kim, P. Yang, O. M. Yaghi, C. J. Chang, *Science*, 2015, **349**, 1208-1213.

2 H.-J. Zhu, M. Lu, Y.-R. Wang, S.-J. Yao, M. Zhang, Y.-H. Kan, J. Liu, Y. Chen, S.-L. Li, Y.-Q. Lan, *Nat. Commun.*, 2020, **11**, 497.

3 Q. Wu, R.-K. Xie, M.-J. Mao, G.-L. Chai, J.-D. Yi, S.-S. Zhao, Y.-B. Huang, R. Cao, *ACS Energy Lett.*, 2020, **5**, 1005-1012.

4 Q. Wu, M.-J. Mao, Q.-J. Wu, J. Liang, Y.-B. Huang, R. Cao, *Small*, 2020, **17**, 2004933.

5 E. M. Johnson, R. Haiges, S. C. Marinescu, *ACS Appl. Mater. Interfacess*, 2018, **10**, 37919-37927.

6 C. S. Diercks, S. Lin, N. Kornienko, E. A. Kapustin, E. M. Nichols, C. Zhu, Y. Zhao, C. J. Chang, O. M. Yaghi, *J. Am. Chem. Soc.*, 2018, **140**, 1116-1122.

7 H. Liu, J. Chu, Z. Yin, X. Cai, L. Zhuang, H. Deng, *Chem.*, 2018, **4**, 1696-1709.

8 X Yang, Q.-X. Li, S.-Y. Chi, H.-F. Li, Y.-B. Huang, R Cao. *SmartMat*, 2022, **3**, 163-172

9 S.-Y. Chi, Q Chen, S.-S. Zhao, D.-H. Si, Q.-J. Wu, Y.-B. Huang, R. Cao. *J Mater Chem A*, 2022, **10**, 4653-4659